This manuscript is contextually identical with the following published paper:

Bruna PaolinelliReis[a1], Sebastião Venâncio Martins[a], Elpídio Inácio Fernandes Filho[b], Tathiane Santi Sarcinelli[c], José MarinaldoGleriani[a], Helio Garcia Leite[a], Melinda Halassy[d] 2019. Forest restoration monitoring through digital processing of high resolution images. Ecological Engineering Volume 127, February 2019, Pages 178-186.

The original published pdf available in this website:

https://doi.org/10.1016/j.ecoleng.2018.11.022

FOREST RESTORATION MONITORING THROUGH DIGITAL PROCESSING OF HIGH RESOLUTION IMAGES

Bruna Paolinelli Reis [a1*]; Sebastião Venâncio Martins [a]; Elpídio Inácio Fernandes Filho [b]; Tathiane Santi Sarcinelli [c]; José Marinaldo Gleriani [a]; Helio Garcia Leite [a]; Melinda Halassy [d]

[a] *Forest Engineer Department. Universidade Federal de Viçosa. Avenida P. H. Rolfs s/n, CEP 36570-000, Viçosa, MG, Brasil.*
[b] *Soil Department. Universidade Federal de Viçosa. Avenida P. H. Rolfs s/n, CEP 36570-000, Viçosa, MG, Brasil.*
[c] *Fibria Celulose S.A. Meio Ambiente Florestal. Rodovia Aracruz - Barra do Riacho, s/n, km 25, Zipcode:29.197-900. Aracruz, ES, Brasil.*
[d] *MTA Centre for Ecological Research, Institute of Ecology and Botany, Alkomány u. 2-4, 2163, Vácrátót, Hungary*

*corresponding author.
E-mail adress: brunapaolinelli@gmail.com (B. P. Reis)

Abstract

Monitoring and evaluating forest restoration projects is a challenge especially in large-scale, but the remote monitoring of indicators with the use of synoptic, multispectral and multitemporal data allows us to gauge the restoration success with more accurately

[1]Permanet address: Eötvös Loránd University, Department of Plant Taxonomy, Ecology and Theoretical Biology, Pázmány P. stny. 1/C, 1117 Budapest, Hungary

and in small time. The objective of this study was to elaborate and compare methods of remote monitoring of forest restoration using Light Detection and Ranging (LIDAR) data and multispectral imaging from Unmanned Aerial Vehicle (UAV) camera, in addition to comparing the efficiency of supervised classification algorithms Maximum Likelihood (ML) and Random Forest (RF). The study was carried out in a restoration area with about 74 hectares and five years of implementation, owned by Fibria Celulose S.A., in the southern region of Bahia State, Brazil. We used images from Canon S110 NIR (green, red, Near Infrared) on UAV and LIDAR data composition (intensity image, Digital Surface Model, Digital Terrain Model, normalized Digital Surface Model). The monitored restoration indicator was the land cover separated in three classes: canopy cover, bare soil and grass cover. The images were classified using the ML and RF algorithms. To evaluate the accuracy of the classifications, the Overall Accuracy (OA) and the Kappa index were used, and the last was compared by Z test. The area occupied by different land cover classes was calculated using ArcGIS and R. The results of OA, Kappa and visual evaluation of the images were excellent in all combinations of the imaging methods and algorithms analyzed. When Kappa values for the two algorithms were compared, RF presented better performance than ML with significant difference, but when sensors (UAV camera and LIDAR) were compared, there were no significant differences. There was little difference between the area occupied by each land cover classes generated by UAV and LIDAR images. The highest cover was generated for canopy cover followed by grass cover and bare soil in all classified images, indicating the need of adaptive management interventions to correct the area trajectory towards the restoration success. The methods employed in this study are efficient to monitor restoration areas, especially on a large scale, allowing us to save time, fieldwork and invested resources.

Keywords: Light Detection and Ranging (LIDAR), Unmanned Aerial Vehicle (UAV), Random Forest (RF), Maximum Likelihood Algorithm, Recovery of Degraded Areas, forest restoration

1. Introduction

Due to the high demand for environmental regularization of big companies and farmers and the need to mitigate environmental impacts generated by human activities, restoration projects have been increased across the globe (Li et al., 2017). The expansion of works and techniques used in restoration initiatives and successive evaluations of what was done in the past made it possible to correct and to adapt the previously used methods to favor functional ecosystem reestablishment (Rodrigues et al., 2009).

Long-term follow-up of large-scale restoration projects is critical because it allows us to evaluate their success or to correct their trajectory through the generation of ecological management recommendations (enrichment, invasive species control, and othres). Therefore, the application of these corrective actions can guarantee the success of the project already in the first years of the planting (Ruiz-Jaen and Aide, 2005; Melo et al., 2013; Zahawi et al., 2015). However, monitoring restoration is a challenge especially in large-scale projects (Viani et al., 2017, Ockendon et al, 2018), mainly because the field assessment of several indicators can be time consuming, costly, and require trained technicians (Zahawi et al., 2015; Reif and Theel, 2017). Additionally, a clear definition of which indicator should be measured and the frequency of assessment still lack (Rodrigues et al., 2009). Alternative approaches to evaluating and monitoring different restoration parameters using remote sensing and digital image processing techniques are considered promising to reduce the need for field measurement methods (Reif and Theel, 2017; Viani et al., 2017), especially for large scale restoration projects and for areas that are difficult to access (Mascaro et al., 2014; Zahawi et al., 2015). Additionally, with the use of remote monitoring it is possible to evaluate restoration in landscape scale, not only in selected samples, as it is usually done in field monitoring (Zahawi et al., 2015).

Land cover composition is an important indicator to evaluate landscape condition and to monitor status and trends of ecosystem change over a specific time (Xian et al., 2009). In our study, land cover indicator was separated in three classes: canopy cover, grass cover and bare soil. According to Harris et al. (2012), canopy cover

93 influences forest structure, amount of light entering the forest, water
94 infiltration, facilitates the growth of understory native seedlings and controls of
95 undesirable grasses, among others. The evaluation of invasive grass cover is considered
96 of high importance in the early stages of the forest restoration process, because these
97 species are spreading rapidly and compete with native species impeding or hindering
98 their growth (Rocha-Nicoleite et al, 2017). Bare soil should be monitored because when
99 it occurs in large spots also compromises the seedlings survival preventing the water
100 infiltration and inducing soil erosion and nutrient loss, among others (Muñoz-Rojas et
101 al., 2016).

102 Out of the new remote sensing techniques that have been widespread Light
103 Detection and Ranging (LIDAR) enables to determine the distance between the sensor
104 and the target surface using laser pulses (Lefsky et al., 2002). Additionally, this sensor
105 is able to generate the pulse return intensity image, which can be useful to classify land
106 cover (Song et al., 2002). According to Giongo et al. (2010) this sensor has proved to be
107 efficient for different forestry applications, since it allows the measurement of canopy
108 topography (Dubayah and Drake, 2000), biomass (Bortolot and Wynne, 2005), volume
109 (Ioki et al., 2010), species identification (Kim et al., 2007; Holmgren et al., 2008) and
110 several other applications. Another remote sensing technique that has been widely used
111 is high-resolution imagery acquired from Unmanned Aerial Vehicle (UAV) camera.
112 Several studies have demonstrated the efficiency of these image processing, e.g. in the
113 mapping of invasive species (Michez et al., 2016), land use and cover planning (Silva
114 et. al., 2016), to monitor tropical forest recovery (Zahawi et al., 2015) and biodiversity
115 (Koh and Wich, 2012; Getzin et al. 2012; Paneque-Galves et al., 2014).

116 Supervised classification is a process of image information extraction where the
117 user selects representative samples of different classes found in the image (Campbell,

1996). A widely used algorithm for image classification is the Maximum Likelihood (ML), which considers the classes involved in a Gaussian probability density function (Hagner and Reese, 2007). Another more robust algorithm that has been shown to be very efficient in the classification of satellite images is the Random Forest (RF) (Gislason et al., 2006; Lawrence et al., 2006; Puissant et al., 2014). This algorithm is based on the generation of multiple decision trees that vote for the most popular class (Breiman, 2001) to produce more accurate classification (Cutler et al., 2007; Puissant, 2014).

The aim of the present study was 1) to elaborate and compare methods of remote monitoring of forest restoration using images from LIDAR data and UAV camera, 2) to compare the efficiency of supervised classification algorithms ML and RF and 3) to obtain land cover composition by classified images.

2. Materials and methods

2.1. Study site

The present study was carried out in conservation areas under restoration process owned by Fibria Celulose S.A., on a farm named "Project Maria Mirreis T734", 39.68° S, 17.71° W, located in the municipality of Caravelas, extreme south of Bahia state, Brazil (Figure 1).

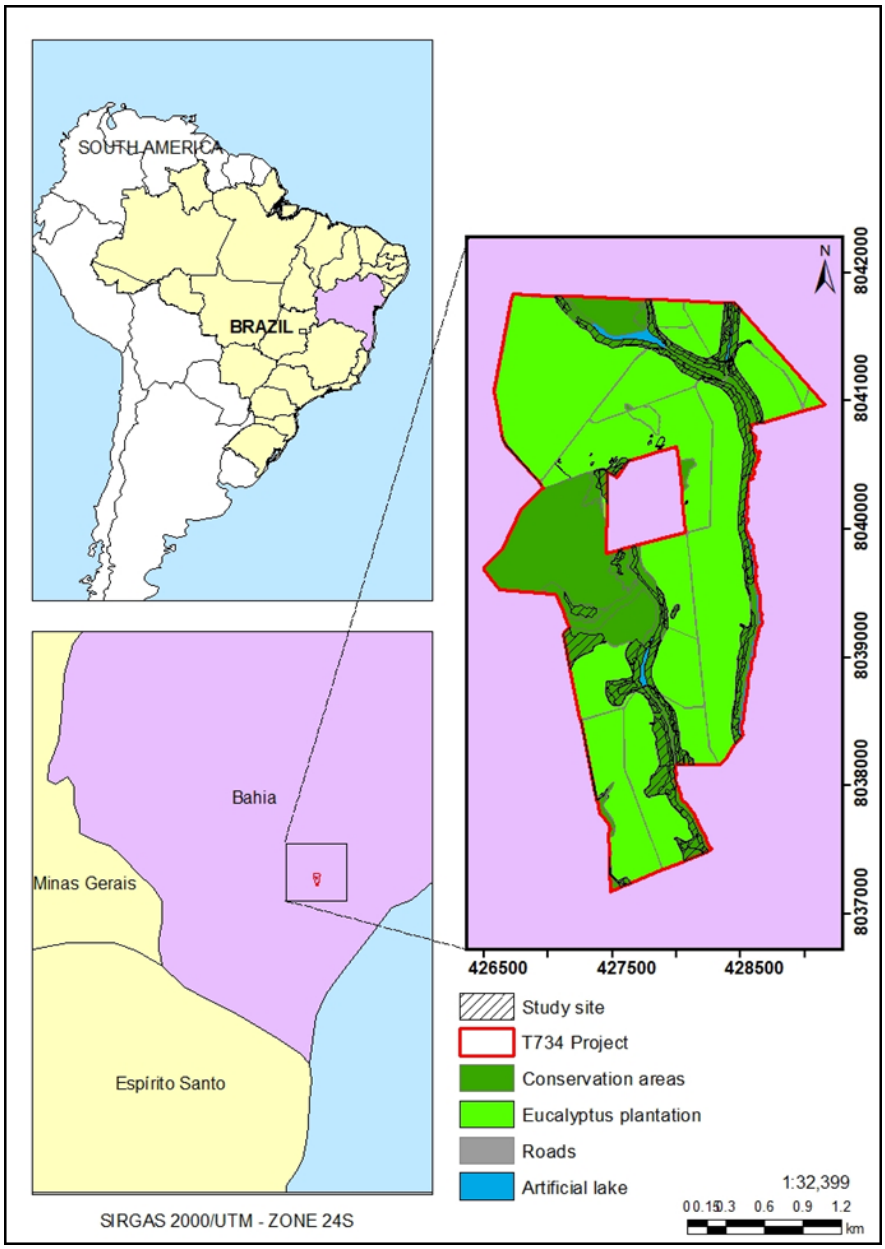

Fig. 1. Location and Land Use of the study site called "Project T734 Maria Mirreis", in south of Bahia state, Brazil.

According to the classification of Köppen, the region is in the transition between Tropical rainforest climate, hot and humid tropical climate on the coast and seazonal climate, with dry winter in the interior (Zonete et al., 2010). The average annual rainfall is around 1,100 mm (Almeida et al., 2008) and the average temperature is 25°C, without defined dry season (Costa et al., 2009). The predominant soils in the region are the kaolinitic Latosols and Yellow or Red-Yellow Argisols, presenting low fertility, and, in

149 case of Argisols, presence of a dense layer in the subsurface (Moreau et al., 2006). The
150 natural vegetation in the region includes Atlantic forests (Dense Ombrophilous Forest
151 and Seasonal Semideciduous Lowland Forests) (Saporetti, 2012).

152 The farm that included our study area has a total area of 664.42 ha, where
153 432.09 ha are planted with eucalyptus, 207.17 ha is conservation areas, 15.78 ha of
154 roads and 9.38 ha for various uses. Among the conservation areas, there are natural
155 forests in different successional stages and degraded pastures dominated by the exotic
156 grass *Urochloa decumbens* (Stapf) R.D.Webste (74 ha). Restoration projects are being
157 carried out mainly in these degraded pastures, which were originally occupied by Dense
158 Ombrofilous forest, and native grasses do not occur (Veloso, 1991; Ivanauskas and
159 Assis, 2012). Aiming to achieve the restoration success, interventions were
160 implemented in 2010 through the methodologies of natural regeneration or planting
161 native species seedling.

162 *2.2. Image gathering from UAV and LIDAR*

163 Aerial images of the study area were obtained from Canon S110 NIR cameras,
164 coupled to UAV in the spring season. The resolution of the images captured by the
165 cameras is 4000 x 3000 pixels, and the spatial resolution is 0.08 meters. The camera
166 captures images in the spectral region of green, red, and near infrared (NIR). The
167 Normalized Difference Vegetation Index (NDVI) (Rouse et al, 1973) (Equation 1) and
168 Soil Adjusted Vegetation Index (SAVI) (Huete, 1988) (Equation 2) were calculated.
169 Then, three spectral bands and two spectral transformations were combined.

170

171 $$NDVI = \frac{(NIR-Red)}{(NIR+Red)}$$ (Equation 1)

172 where: *NIR* = Near Infrared band and Red = Red band

173

$$SAVI = \frac{(1+Ls)*(NIR-Red)}{(Ls+NIR+Red)} \quad \text{(Equation 2)}$$

where: *Ls* is a constant denominated factor of adjustment of the SAVI index, being able to assume values from 0.25 to 1 depending on the land cover. In this case, the value of 0.5 was considered, representing vegetation with intermediate density (Huete, 1988)

Images were also obtained through a RIEGL LMS - Q680I Airborne Laser system denominated LIDAR, which works on Near Infrared region with a wavelength of 1,036 nm. The images were taken in spring season. From LIDAR point clouds, it was possible to generate the pulse return intensity image, Digital Surface Model (DSM), Digital Terrain Model (DTM) and normalized Digital Surface Model (nDSM) using ArcGIS 10.2 (ESRI, 2015). nDSM stores information of the objects height, obtained through the difference between DSM and DTM. According to Song et al. (2002), the intensity is defined as the ratio of strength of reflected light to the emitted light and can be useful to classify the land cover. By using the obtained data, a 0.5 m spatial resolution image composed of four bands (Intensity, nDSM, DTM, DSM) was generated. Thus, in addition to the information of the vegetation height, there is also the spectral information related to the pulse return intensity.

2.3.Land cover monitoring

The monitored restoration indicator was the land cover separated in three classes: canopy cover, bare soil and grass cover. These classes were chosen due to the feasibility for obtaining results from aerial images classification. All these classes are easily identified by visual image interpretation and digital image processing due to clear differences between their spectral signatures. They also have ecological importance in early stages of restoration process and relevance for generating adaptive management

199 recommendations, which aim to correct the trajectory of a restoration area allowing its
200 ecological succession (Atlantic Forest Restoration Pact, 2013; Viani et al., 2017).
201 UAV camera is a passive sensor, which requires sunlight as an illumination
202 source for obtaining images. Therefore, the presence of clouds and shadows modifies
203 the reflectance of the objects and can reduce the classification accuracy. For this reason,
204 besides the three mentioned classes, it was necessary to establish another class
205 representing objects in shadows, which was called "shadow".
206
207 *2.4. Sample selection, classification, accuracy, comparison and class area*
208 *quantification*
209 Fifty representative samples of each class (canopy cover, bare soil and grass
210 cover, shadow) were selected over UAV camera images. The same number of samples
211 per class (canopy cover, bare soil and grass cover) were chosen over LIDAR return
212 intensity channel. These samples were polygons with the same size, 450 pixels on
213 average for the UAV camera images and 55 pixels for LIDAR images due to the
214 different spatial resolution between both sensors. The software ArcGIS 10.2 (ESRI,
215 2015) was used for sample acquisition. Seventy percent of the samples polygons were
216 randomly selected for training and thirty percent them was left for validation of both
217 algorithms (ML and RF).
218 The supervised classification using ML algorithm was done with ArcGIS 10.2
219 software, whereas the RF algorithm was done with R 3.3.2 software (R Core Team,
220 2016). The fifty samples used for classification were randomly divided into training and
221 validation samples ten times, and for each division classification models were fitted. RF
222 algorithm also permitted to generate the variable importance, which represents the most

223 important variables for creating algorithm's decision trees, through two methods:
224 randomization and Gini Index, described by Hastie et al. (2009).

225 Thirty percent of the selected samples from UAV and LIDAR images were used
226 for the validation phase to verify the accuracy of the methods. The classification
227 accuracy was assessed with the confusion matrix approach. From this matrix,
228 classification accuracy indicators, such as Producer's accuracy, User's accuracy,
229 Overall classification accuracy, and Kappa coefficient, were calculated. Additionally,
230 ten samples of each class were collected in the field, totaling 30 validation samples, and
231 the coordinates of each sampling point was obtained with GPS. This sampling was done
232 to evaluate whether the sampling on UAV and LIDAR images may have some bias that
233 leads to over or underestimated accuracy. After obtaining the Kappa Index, it was
234 possible to classify its value according to the literature (Landis and Kock, 1977).

235 As it was mentioned before 10 classifications were performed by each
236 combination between imaging method and algorithm, therefore we calculate the average
237 of Producer's accuracy, User's accuracy, Overall classification accuracy, and Kappa
238 coefficient, in each situation. The Z test was used to compare Kappa values among all
239 different classified images with a 95% confidence level, $Z > 1.96$ (Foody, 2004;
240 Congalton and Green, 2009).

241 We calculated the land cover composition based on percentage class area
242 (canopy cover, grass cover, bare soil and shadow) generated by the most accurate
243 classification (from the 10 classifications), for each classified image using ArcGIS
244 software (ESRI, 2015) and R software (R Core Team, 2016) for ML and RF,
245 respectively.

The complete procedure that we used to classify UAV and LIDAR images with different classifying algorithms and the validation performed to verify the classifiers accuracy is presented in Figure 2.

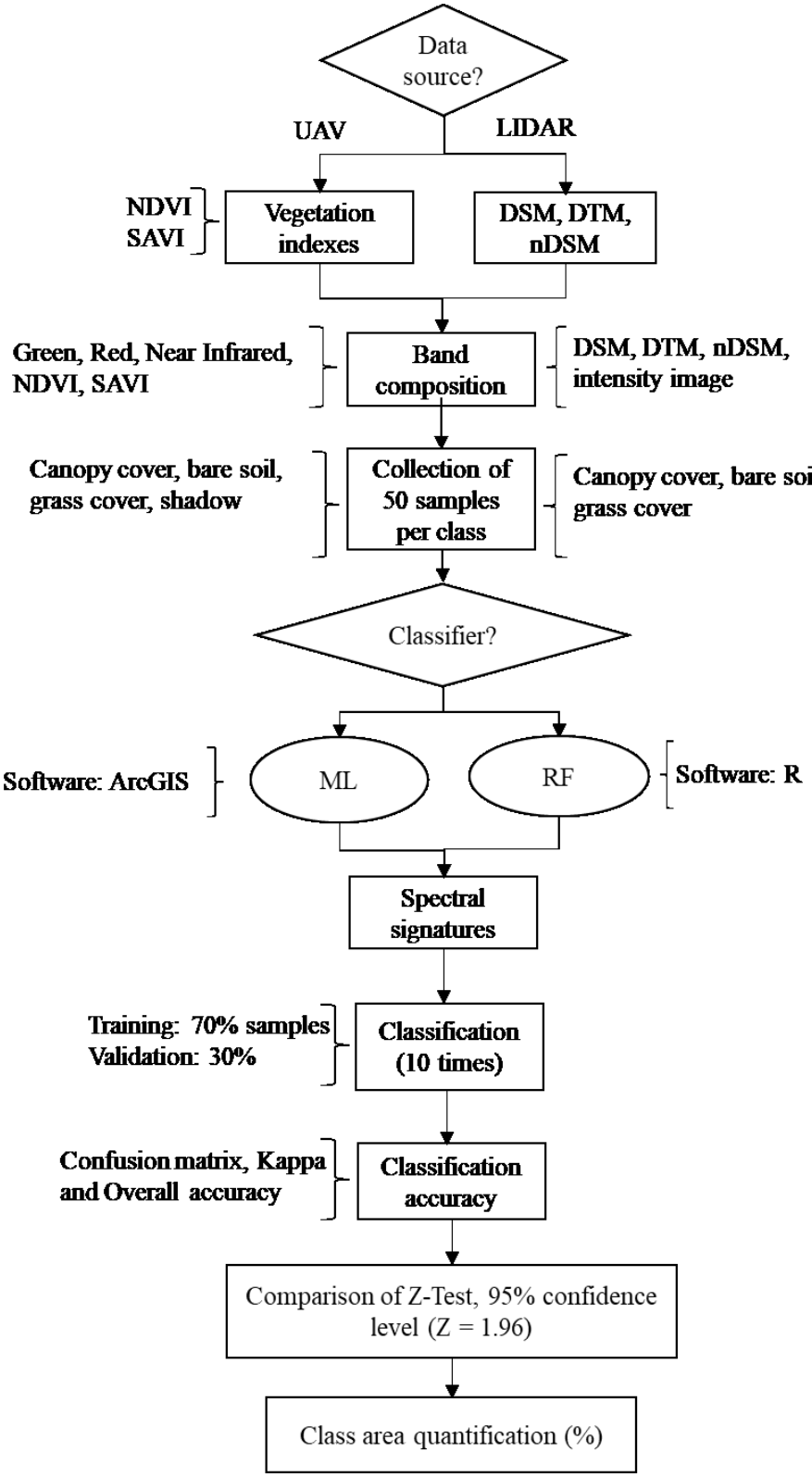

Fig 2. Flowchart representing the methodology used to classify LIDAR and UAV images, using the ML and RF algorithms, and the accuracy of the classifications. DTM: Digital Terrain Model, DSM: Digital Surface Model, LIDAR: Light Detection and Ranging, ML: Maximum Likelihood, nDSM: normalized Digital Surface Model, NDVI: Normalized Difference Vegetation Index, RF: Random Forest, SAVI: Soil Adjusted Vegetation Index, UAV: Unmanned Aerial Vehicle.

3. Results

3.1. Classification by the Maximum Likelihood and Random Forest algorithms from UAV camera images

The images obtained by UAV camera classified using ML and RF algorithms is presented in Figure 3, and it represents part of the restoration project.

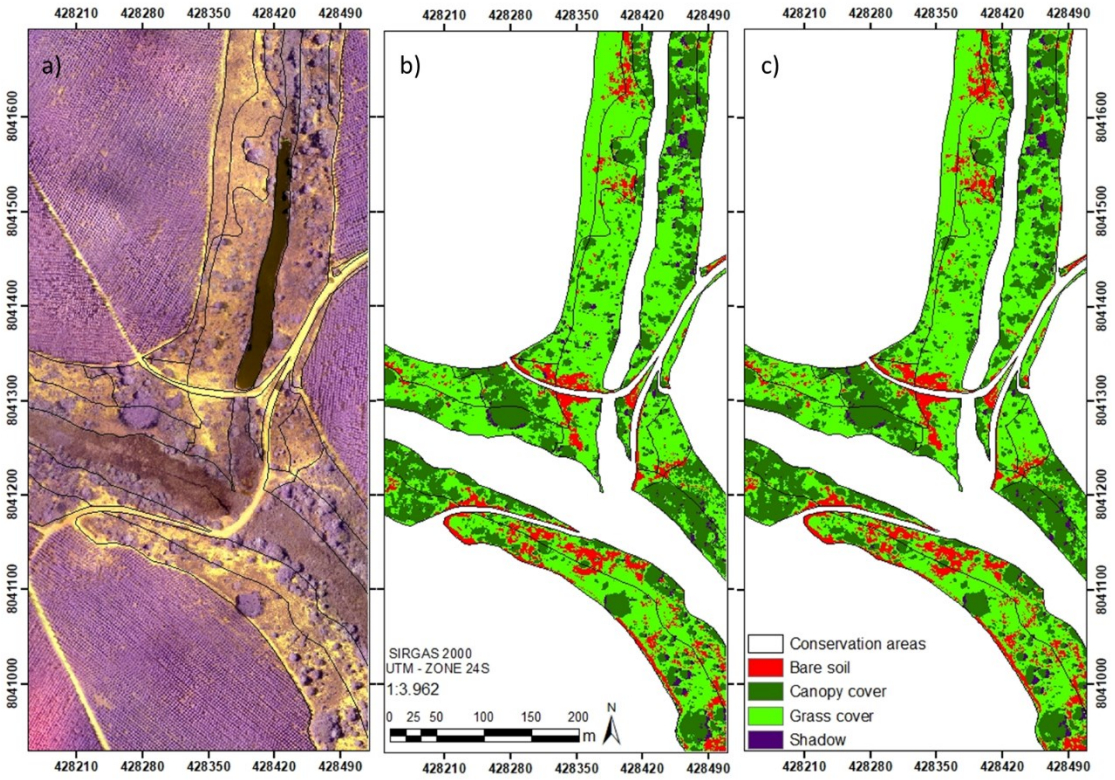

Fig. 3. a) UAV camera images (Red, Green, Near Infrared, NDVI, SAVI), which represent part of the study area; b) Image classified by Maximum Likelihood algorithm; c) Image classified by Random Forest algorithm.

It is noticed that all the classes were well delimited on UAV classified images by both algorithms and they were quite similar (Fig.3).

The Tables 1 and 2 represents the mean values generated from the ten confusion matrices for both classifiers. It was observed that Kappa and Overall Accuracy were

high and ranked as excellent (Landis and Kock, 1977) for both algorithms. The classes separation was also assessed through user's and producer's accuracy. The values of these indices were high in both classifications, indicating a good level of discrimination between classes. Additionally, "shadow" was the class that most generates confusion, especially with "bare soil" and "grass cover" for both classifiers.

Table 1
Mean values generated from the ten confusion matrices, with the Maximum Likelihood classifier, for UAV camera images

CLASS	Bare Soil	Canopy cover	Grass cover	Shadow	Total	PA (%)
Bare soil	**6463**	3	91	388	6945	93.17
Canopy cover	0	**8097**	184	94	8375	96.75
Grass cover	21	65	**7929**	440	8455	94.02
Shadow	376	282	114	**3858**	4630	81.55
Total	6860	8447	8318	4779	**28404**	
UA (%)	96.21	96.45	95.63	90.00		
Average Kappa					0.90	
Average OA					0.93	

OA: Overall Accuracy, PA: Producer's Accuracy, UA: User's Accuracy.

Table 2
Mean values generated from the ten confusion matrices, with the Random Forest classifier, for UAV camera images

CLASS	Bare Soil	Canopy cover	Grass cover	Shadow	Total	PA (%)
Bare soil	**6408**	3	43	0	6454	99.34
Canopy cover	1	**6992**	109	1	7103	98.65
Grass cover	186	244	**5836**	172	6438	89.43
Shadow	1	80	63	**2493**	2637	93.88
Total	6596	7319	6051	2666	**22632**	
UA (%)	96.46	95.35	96.84	93.12		
Average Kappa					0.94	
Average OA					0.96	

OA: Overall Accuracy, PA: Producer's Accuracy, UA: User's Accuracy.

From the ten generated confusion matrices, the minimum Kappa value found with ML algorithm was 0.69, and the maximum value was 0.99, with a mean of 0.90

and a standard deviation of 0.094. For RF, the minimum Kappa value found was 0.85 and the maximum was 0.99, with a mean of 0.94 and a standard deviation of 0.043.

A significant difference was verified by the Z test ($Z > 1.96$ at 95% of confidence level) (Table 5) among Kappa values for each classifier. In addition, RF algorithm presented the best Kappa and OA results, being considered the best alternative for image processing.

When validation was performed using the field samples, the Kappa indexes remained in the excellent range for both algorithms, 0.97 for ML and RF. The OA was also considered high (0.98 for both algorithms), proving that the field data are consistent with the results obtained through training and validation when using samples selected in the image itself.

The variables importance generated by the RF for UAV image, in decreasing order, were red band, green, SAVI, NDVI and near infrared.

3.2. Classification using Maximum Likelihood and RF algorithms from LIDAR data composition images

The images obtained by LIDAR data composition, classified using ML and RF algorithms is presented in Figure 4, and it represents part of the restoration project.

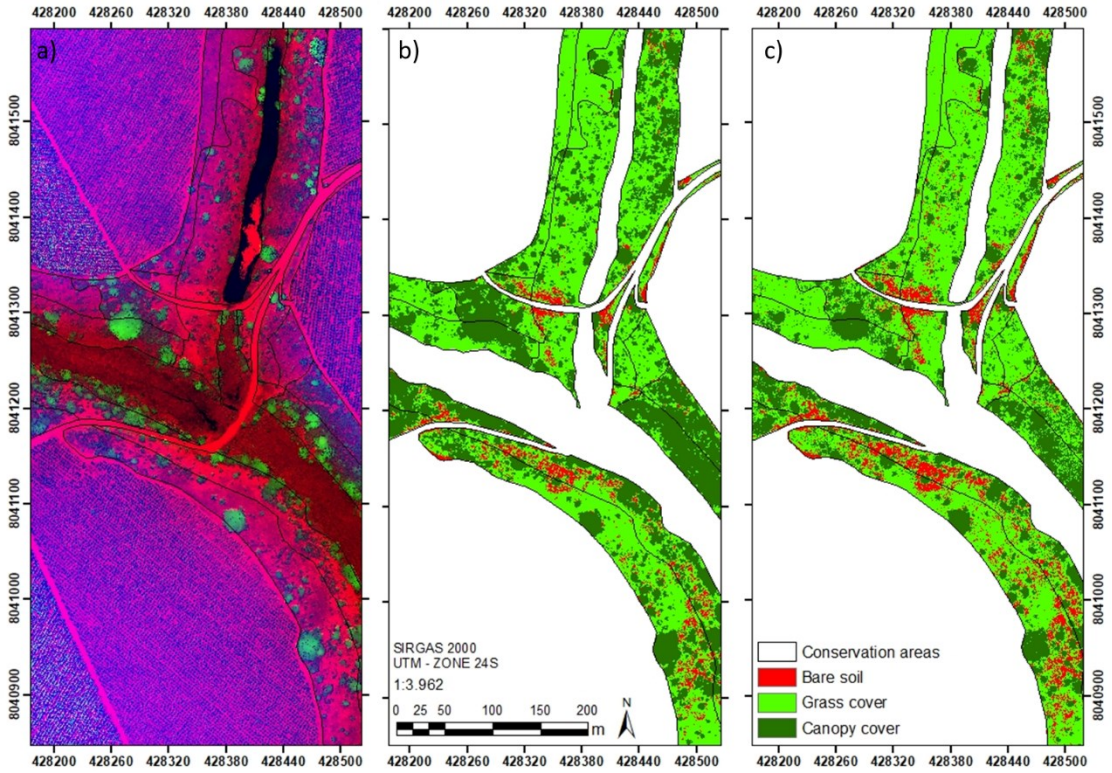

Fig. 4. a) LIDAR data composition images (Intensity, nDSM, DSM, DTM); b) Image classified by Maximum Likelihood algorithm; c) Image classified by Random Forest algorithm.

It is noticed that all the classes were well delimited on classified LIDAR images by both algorithms and they were quite similar (Fig.4).

According to Tables 3 and 4, Kappa and Overall Accuracy were high and ranked as excellent (Landis and Kock, 1977). User's and producer's accuracy values were also considered high for both algorithms indicating few confusions among classes. The greatest confusion was between "bare soil" and "grass cover" for both classifiers.

Table 3

Mean values generated from the ten confusion matrices, with the Maximum Likelihood classifier, for LIDAR data images

CLASS	Bare soil	Grass cover	Canopy cover	Total	PA (%)
Bare soil	**817**	0	1	817	99.38
Grass cover	62	**557**	31	649	86.16
Canopy cover	72	8	**678**	758	89.50
Total	950	565	710	**2225**	
UA (%)	89.24	98.32	96.12		
Average Kappa				0.88	
Average OA				0.92	

OA: Overall Accuracy, PA: Producer's Accuracy, UA: User's Accuracy.

Table 4

Mean values generated from the ten confusion matrices, with the Random Forest classifier, for LIDAR data images

CLASS	Bare soil	Grass cover	Canopy cover	Total	PA (%)
Bare soil	**493**	14	0	507	97.29
Grass cover	53	**595**	1	649	92.13
Canopy cover	0	0	**642**	642	100
Total	547	608	643	**1798**	
UA (%)	91.80	97.77	99.85		
Average Kappa				0.94	
Average OA				0.96	

OA: Overall Accuracy, PA: Producer's Accuracy, UA: User's Accuracy.

The minimum Kappa value found with ML was 0.61, and the maximum value was 0.98, with a mean of 0.88 and a standard deviation of 0.14. For RF, the minimum Kappa was 0.76, and the maximum was 0.98, with a mean of 0.94 and a standard deviation of 0.07.

A significant difference was verified by the Z test ($Z > 1.96$ at 95% of confidence level) (Table 5) among the Kappa values for each classifier. RF algorithm presented the best Kappa and OA results, then this algorithm was considered the best alternative for LIDAR images processing.

When field samples were used to validate the classifications, the Kappa Index remained in the excellent range, 0.86 for ML algorithm and 0.95 for RF. The OA was

343 also considered high, with 0.91 and 0.97 for ML and RF, respectively, proving that field
344 data are consistent with the results obtained through training and validation, using
345 samples collected in the image itself.

346 The variables importance generated by RF for LIDAR image, in decreasing
347 order, were intensity band, nDMS, DSM and DTM.

348

349 *3.3 Comparison between imaging methods: LIDAR and UAV camera*

350 Considering that the best classification result was obtained using RF algorithm,
351 LIDAR and UAV methods were compared first for that algorithm. The difference
352 between LIDAR and UAV methods was nonsignificant ($Z < 1.96$ at 95% of confidence
353 level) (Table 5), demonstrating that method selection does not significantly affect the
354 results. On the other hand, when using ML, a significant difference ($Z > 1.96$ at 95% of
355 confidence level) (Table 5) was found between LIDAR and UAV images
356 classifications. In this case, the image from UAV camera produced a higher accuracy
357 classification.

358 Table 5 is a summary of Kappa and Z test values for each method evaluated on
359 this study.

360 **Table 5.** Kappa Index found for UAV and LIDAR images classified by Maximum
361 Likelihood and Random Forest algorithms. The Table also presents the Z values for
362 comparison among the algorithm (RF and ML) for each imaging methods (UAV and
363 LIDAR), and the comparison between imaging methods (LIDAR and UAV) for each
364 algorithm (RF and ML)

Kappa Values	ML	RF	Z test ML x RF
UAV	0.90	0.94	14.55*
LIDAR	0.88	0.94	5.74*
Z test UAV x LIDAR	2.58*	0.06	

365

366 * Significant difference ($Z > 1.96$ at 95% of confidence level). LIDAR: Light Detection
367 and Ranging, ML: Maximum Likelihood; RF: Random Forest; UAV: Unmanned Aerial
368 Vehicle.

3.4 Land cover composition obtained by classified images

The area covered by canopy, grass and bare soil in the studied project generated through different image classification methods is represented in Figure 5. The highest percentage cover was generated for canopy cover followed by grass cover and bare soil in all classified images.

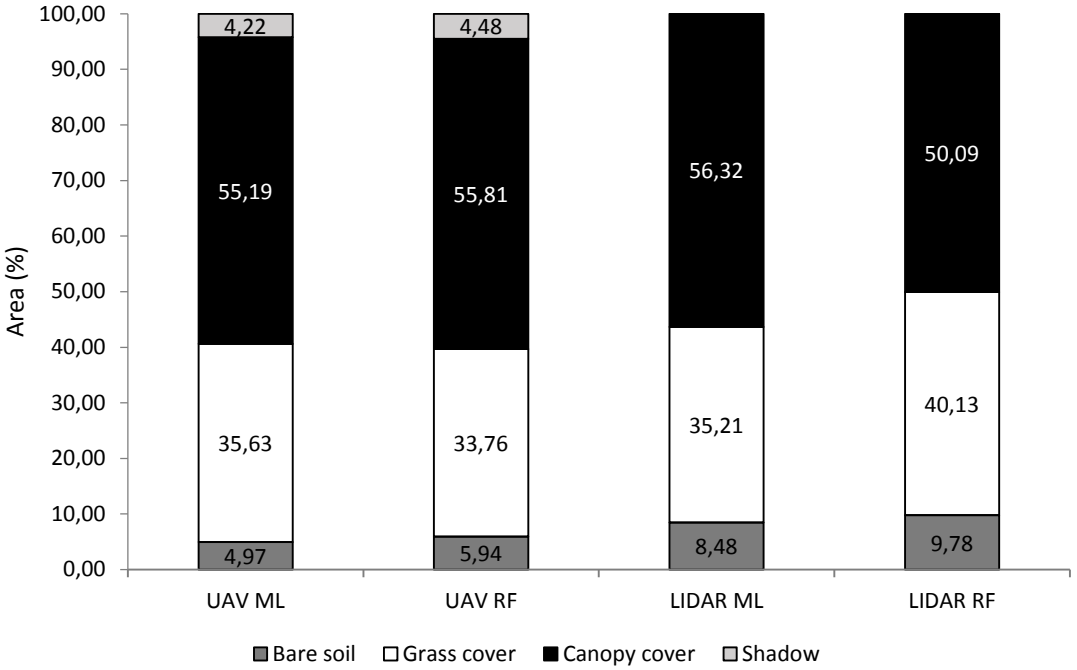

Fig. 5. Percentage area for canopy cover, grass cover and bare soil found through different image classification methods: UAV camera images classified with ML and RF algorithms, LIDAR images classified with ML and RF algorithms. LIDAR: Light Detection and Ranging, ML: Maximum Likelihood; RF: Random Forest; UAV: Unmanned Aerial Vehicle.

4. Discussion

We elaborated and compared methods of remote monitoring of forest restoration using LIDAR data and multispectral imaging of UAV camera and compared the efficiency of supervised classification algorithms ML and RF that proved to be reliable tools for assessing land cover composition. Field monitoring and evaluation of restoration requires a great deal of efforts mainly in large-scale projects (Zahawi et al., 2015; Reif and Theel, 2017; Ockendon et al, 2018), but the use of remote monitoring of

389 land cover indicators with synoptic, multispectral and multitemporal data (Paneque-
390 Galves et al., 2014; Reif and Theel, 2017) allow us to save time, fieldwork and
391 resources (Zahawi et al., 2015).
392
393 *4.1 Comparison between algorithms: Maximum Likelihood and Random Forest*
394 As previously mentioned, Kappa index and OA were chosen to evaluate the
395 accuracy of the classification since those measures are still the most used in image
396 classification, although they have recently been questioned (Lyons et al., 2018). Similar
397 values of Kappa and OA were found in all classifications and these values were also
398 high, denoting the classifier precision.
399 Although Kappa values were similar and ranked as excellent in all combinations
400 of images and algorithms, RF presented higher values of accuracy than the ML. This is
401 in accordance with studies carried out by Gislason et al. (2006), which RF efficiency
402 (Overall Accuracy = 82.8%) proved to be better when compared with other classifiers
403 (ensemble methods and CART - decision trees) for land cover classification with an
404 image composition (Landsat satellite images, elevation, slope and aspect) in Colorado.
405 RF algorithm has been widely used by ecologists because of its simple interpretation,
406 high accuracy, rapid processing, robustness to outliers and noises and ability to
407 characterize complex interactions between variables (Breiman, 2011; Cutler et al.,
408 2007).
409 An interesting feature of RF classification is the possibility of obtaining the
410 variables importance, especially in situations where it is necessary to classify
411 hiperspectral images (Gislason et al., 2006). In our study with multispectral images,
412 intensity band and nDSM were the most important variables of LIDAR image
413 classification. This can be justified by the fact that intensity band has spectral

414 information and nDSM has height information, in other words, they are poorly
415 correlated, providing less redundant data for the classifier (Lu and Weng, 2007). For
416 UAV images, the most important variables were the red and green bands, followed by
417 SAVI index, which also are the less correlated variables of the composition.

418 Although the ML algorithm was slightly less assertive than the RF, it also
419 presented results ranked as excellent, which makes it eligible for this type of
420 monitoring. This classifier is widely used for remote sensing, displaying good results
421 when the data have a normal distribution and when sample selection represents well the
422 spectral diversity of the class to be mapped (de Oliveira et al., 2013). ML has already
423 proved efficient in several studies, such as the study by Silva et al. (2016), who tested
424 the efficiency of this classifier, after segmentation, for monitoring Brazilian Savanna
425 (*Cerrado)* land cover with UAV image, and obtained high values of similarity (0.94)
426 with the visual interpretation. In the case of de Oliveira et al. (2013), who mapped forest
427 fragments with monodominant *aroeira* (*Myracrodruon urundeuva*), ML classifier
428 presented the best performance (Kappa = 80) in RapidEye images classification when
429 compared to Neural Networks.

430

431 *4.2 Comparison between imaging methods: LIDAR and UAV camera*

432 No significant difference was found when comparing the sensors (LIDAR or
433 UAV camera) using RF algorithm. Therefore, regardless the method choice, good
434 results are expected to be obtained when RF is used. In case of ML, there was
435 significant difference between the methods, so UAV images presented better results
436 than LIDAR.

437 The "shadow" class was the one that mostly generated confusion in UAV
438 camera images for both classifiers. This confusion can be justified by the fact that

shadows cause partial or total loss of radiometric signature in the analyzed areas thus this can affect the performance of image classification process, object identification and consequently the land-cover mapping (Adeline et al., 2013; Movia et al., 2016). Shadow in images can be considered as a disadvantage of the use of UAV camera images when compared to LIDAR. The latter is considered an active sensor that have their own light source and does not require sunlight, so shadow interference does not occur in images (Song et al, 2002; Giongo et al., 2010) reducing the probability of class confusions in classification.

Little confusion was found between the classes when LIDAR data were evaluated. In this case, the greatest confusion was between bare soil and grass cover. In a study conducted by Song et al. (2002) using LIDAR, it was found that only with intensity band it would be difficult to separate grass cover from canopy cover, but with the addition of nDSM band, this becomes possible. According to Thenkabail et al. 2004, an increase in spectral bands quantity may improve the accuracy of classification, but only when these bands are useful for discriminating the classes. The low spectral information of the analyzed images does not show an adverse influence on the classifications since both Kappa and OA values were high, with few confusing errors. However, selecting samples within LIDAR images was more difficult since the small number of spectral bands hinder the visual differentiation among classes.

The use of LIDAR has been shown to be efficient for forest applications because it mobilizes many points with high precision, low cost and high speed of data acquisition (Giongo et al., 2010). Additionally, LIDAR data has already been proved to be successful (Overall Accuracy = 75%) for grassland habitats classification with RF algorithm as showed on the study developed by Zlinszky et al. (2014) in Hungary. According to data provided by Fibria and to Zahawi et al., 2015, the use of LIDAR is

464 more financially feasible for large areas. On the other hand, UAV is feasible for small
465 area imaging (Paneque-Galves et al., 2014; Zahawi et al., 2015).
466 To achieve better results on remote monitoring and make the evaluation of a
467 greater number of indicators possible, such as arboreal individual density, species
468 richness, invasive tree cover and vegetation strata, it is suggested the use of aerial
469 cameras with high resolution and LIDAR sensor coupled, or Ecosynth (new aerial
470 remote sensing system with similar properties to LIDAR, but with RGB spectral
471 attributes for each point, e.g. Zahawi et al., 2015). In this case, in addition to increase
472 spectral information, there will be geometry data (Persson et al., 2004). Additionally,
473 the use of region-based image classification, through segmentation of images it is
474 suggested to improve accuracy values. In the study carried out by Holmgren et al.
475 (2008) in Scandinavia to identify local occurrence of species, higher value of OA (96%)
476 was found when segmentation was used before the classification of aerial camera
477 images combined with LIDAR data by the ML algorithm. The combination of both
478 devices allows us to evaluate a greater number of indications with high accuracy, but it
479 makes the monitoring process more expensive.
480
481 *4.3 Land cover composition by classified images*
482 Slight variations in the area occupied by different classes were observed between
483 the image classification methods. These little variations may be associated with the
484 presence of shaded areas in UAV camera images (cf. Adeline et al., 2013; Movia et al.,
485 2016), that probably consist of bare soil or grass in the field or, additionally, by wrongly
486 classified pixels in the digital image processing.
487 The highest cover was generated for canopy cover by all methods, followed by
488 grass cover and then bare soil. According to the Atlantic Forest Restoration Pact (2013)

and Viani et al. (2017), after four years of restoration implementation the canopy cover should achieve at least 70% to be capable to reduce invasive grass cover and to facilitate tree establishment. Our study area has not reached the desired value yet, probably due to the planting methodology, which used lines of early seral tree species interspersed with late seral species that have slower development and higher mortality. The high grass cover found in this study can be explained by the fact that the project area was covered by degraded pastures dominated by *Urochloa decumbens* before restoration activities and by the short time period since the restoration process has started. The invasive grass cover also competes with native tree seedlings species impeding or hindering their growth (Rocha-Nicoleite et al, 2017), and this can be seen in our restoration area. Bare soil cover was not high, but when it occurs in large areas, it induces soil erosion and nutrient loss (Muñoz-Rojas et al., 2016) that call for further restoration interventions.

According to the Atlantic Forest Restoration Pact (2013) and Viani et al. (2017), after checking the land cover indicators, a field ecological monitoring (phase II) has to be done in areas where canopy cover is greater than 70%. This monitoring is to verify species composition indicators (e.g. richness, density, regeneration) based on field sampling and it will guide adaptive management techniques aiming to correct the restoration trajectory of the areas if necessary. This two-step evaluation (remote sensing and field monitoring) should reduce the costs associated with monitoring, since it will not be necessary to measure field indicators in all areas. The field study related to this monitoring will be presented in a future paper.

5. Conclusions

The methods employed in this study are efficient to monitor restoration areas, bringing gains in quality and precision, synoptic analysis and reduction of field efforts,

514 especially on a large scale. RF algorithm presented the greatest assertiveness in the
515 image classification by UAV camera and LIDAR. The land cover composition found on
516 this research suggests that the study area has not achieved the restoration success yet,
517 therefore adaptive management strategies must be adopted to correct their trajectory
518 towards the desired target state for restoration projects.
519
520 **Acknowledgments**
521 The authors of this study thank Fibria Celulose S.A. for providing the data and
522 financial support and the National Council for Scientific and Technological
523 Development (CNPq) for granting the first author's Master's scholarship and research
524 productivity for the second author.
525
526 **References**
527
528 Adeline, K. R. M., Chen, M., Briottet, X., Pang, S. K., Paparoditis, N., 2013. Shadow
529 detection in very high spatial resolution aerial images: A comparative
530 study. ISPRS Journal of Photogrammetry and Remote Sensing, 80, 21-38.
531 DOI:10.1016/j.isprsjprs.2013.02.003
532 Almeida, T.M., Moreau, A. M.S.S., Moreau, M.S., Pires, M.D.M., Fontes, E.D.O.,
533 Góes, L. M., 2008. Reorganização socioeconômica no extremo sul da Bahia
534 decorrente da introdução da cultura do eucalipto. Sociedade & Natureza, 20 (2),
535 5-18. (Abstract in English). http://dx.doi.org/10.1590/S1982-
536 45132008000200001
537 Atlantic Forest Restoration Pact (Pacto pela Restauração da Mata Atlântica). Protocolo
538 de Monitoramento para Programas e Projetos de Restauração Florestal
539 (Monitoring Protocol for Forest Restoration Projects). 2013. Available in:
540 <http://media.wix.com/ugd/5da841_c228aedb71ae4221bc95b909e0635257.pdf>
541 . Accessed in: 3 Jul. 2017.

542 Bortolot, Z.J., & Wynne, R.H., 2005. Estimating forest biomass using small footprint
543 LIDAR data: An individual tree-based approach that incorporates training
544 data. ISPRS Journal of Photogrammetry and Remote Sensing, 59 (6), 342-360.
545 DOI:10.1016/j.isprsjprs.2005.07.001
546 Breiman, L. 2001. Random forests. Machine Learning, 45, 15–32.
547 Campbell, J. B., 1996. Introduction to remote sensing. New York: The Guilford Press,
548 622 p.
549 Cutler, R., Edwards, T.C., Beard, K.H. Cutler, A., Hess, K.T., Gibson, J., Lawler, J.J.,
550 2007. Random Forests for classification in ecology. Ecology, 88 (11), 2783-
551 2792. DOI:10.1890/07-0539.1
552 Costa, O.V., Cantarutti, R.B., Fontes, L.E.F., Costa, L.D., Nacif, P.G.S., Farias, J.C.,
553 2009. Estoque de carbono do solo sob pastagem em área de tabuleiro costeiro no
554 sul da Bahia. Revista Brasileira de Ciência do Solo, 33 (5), 1137-1145. (Abstract
555 in English). http://dx.doi.org/10.1590/S0100-06832009000500007
556 Congalton, R., Green, K., 2009. Assessing the accuracy of remotely sensed data:
557 Principles and Practices. Boca Raton: CRC Press, Taylor & Francis Group, 183
558 p.
559 Dubayah, R.O., Drake, J.B., 2000. LIDAR Remote Sensing for Forestry. Journal of
560 Forestry, 98, 44-46. https://doi.org/10.1093/jof/98.6.44
561 ESRI, Environmental Systems Research Institute, 2015. ArcGIS for Desktop. Version
562 10.3. Redlands, California, United States.
563 Foody, G.M., 2004. Thematic map comparison: evaluating the statistical significance of
564 differences in classification accuracy. Photogrammetric Engineering & Remote
565 Sensing, 70 (5), 627-633. http://dx.doi.org/10.14358/PERS.70.5.627
566 Getzin, S., Wiegand, K., Schoening, I., 2012. Assessing biodiversity in forests using
567 very high-resolution images and Unmanned Aerial Vehicles. Methods in
568 Ecology and Evolution. 3, 397-404. DOI: 10.1111/j.2041-210X.2011.00158.x
569 Giongo, M., Koehler, H. S., do Amaral Machado, S., Kirchner, F.F., Marchetti, M.,
570 2010. LIDAR: princípios e aplicações florestais. Pesquisa Florestal
571 Brasileira, 30 (63), 231. (Abstract in English). DOI: 10.1111/j.2041-
572 210X.2011.00158.x
573 Gislason, P.O., Benediktsson, J. A., Sveinsson, J. R., 2006. Random forests for land
574 cover classification. Pattern Recognition Letters, 27 (4), 294-300.
575 DOI:10.1016/j.patrec.2005.08.011

576 Hagner, O., Reese, H., 2007. A method for calibrated maximum likelihood
577 classification of forest types. Remote sensing of environment, 110(4), 438-444.
578 https://doi.org/10.1016/j.rse.2006.08.017
579 Harris, C. J., Leishman, M. R., Fryirs, K. and Kyle, G., 2012. How Does Restoration of
580 Native Canopy Affect Understory Vegetation Composition? Evidence from
581 Riparian Communities of the Hunter Valley Australia. Restoration Ecology, 20:
582 584–592. DOI:10.1111/j.1526-100X.2011.00823.x
583 Hastie, T., Tibshirani, R., Friedman, J., 2009. The elements of statistical learning: data
584 mining, inference, and prediction. Springer New York: Springer Series in
585 Statistics, 758p.
586 Holmgren J., Persson Å., Söderman U., 2008. Species identification of individual trees
587 by combining high resolution LIDAR data with multi spectral images,
588 International Journal of Remote Sensing, 29 (5), 1537-1552. DOI:
589 10.1080/01431160701736471
590 Huete, A.R. A soil adjusted vegetation index (SAVI), 1988. Remote Sensing of
591 Enviroment, 25 (3), 295-309. https://doi.org/10.1016/0034-4257(88)90106-X
592 Ioki, K., Imanishi, J., Sasaki, T., Morimoto, Y., Kitada, K., 2010. Estimating stand
593 volume in broad-leaved forest using discrete-return LIDAR: plot-based
594 approach. Landscape and Ecological Engineering, 6 (1), 29-36. DOI:
595 10.1007/s11355-009-0077-4
596 Ivanauskas, N. M., Assis, M.C., 2012. Formações florestais brasileiras. In: Martins,
597 S.V., (Org.). Ecologia de Florestas Tropicais do Brasil. 2ed.Viçosa-MG: Editora
598 UFV, v. 1, p. 01-371.
599 Kim, S., McGaughey, R.J., Andersen, H.E., Schreuder, G., 2009. Tree species
600 differentiation using intensity data derived from leaf-on and leaf-off airborne
601 laser scanner data. Remote Sensing of Environment, 113 (8), 1575-1586. DOI:
602 10.1016/j.rse.2009.03.17
603 Koh, L. P., Wich, S. A., 2012. Dawn of drone ecology: low-cost autonomous aerial
604 vehicles for conservation. Tropical Conservation Science, 5(2):121-132.
605 Available online: www.tropicalconservationscience.org
606 Kopen
607 Landis, J., Koch, G.G., 1977. The measurements of agreement for categorical data.
608 Biometrics, 33 (1), 159-174. DOI: 10.2307/2529310

609 Lawrence, R.L., Wood, S.D., Sheley, R.L., 2006. Mapping invasive plants using hyper-
610 spectral imagery and Breiman Cutler classifications (Random Forest). Remote
611 Sensing of Environment, 100, 356–362. DOI: 10.1016/j.rse.2005.10.014
612 Lefsky, M. A., Cohen, W. B., Parker, G.G., Harding, D. J., 2002. LIDAR remote
613 sensing for ecosystem studies. BioScience, v. 52, n. 1, p. 19-30.
614 http://dx.doi.org/10.1641/0006-3568(2002)052[0019: LRSFES]2.0.CO;2
615 Li, T., Lü, Y., Fu, B., Comber, A. J., Harris, P., & Wu, L. (2017). Gauging policy-
616 driven large-scale vegetation restoration programmes under a changing
617 environment: Their effectiveness and socio-economic relationships. Science of
618 the Total Environment, 607, 911-919.
619 http://dx.doi.org/10.1016/j.scitotenv.2017.07.044
620 Lu, D., Weng Q., 2007. A survey of image classification methods and techniques for
621 improving classification performance. International Journal of Remote Sensing,
622 28 (5), 823-870. DOI: 10.1080/01431160600746456
623 Lyons, M. B., Keith, D. A., Phinn, S. R., Mason, T. J., Elith, J., 2018. A comparison of
624 resampling methods for remote sensing classification and accuracy
625 assessment. Remote Sensing of Environment, 208, 145-153.
626 Mascaro, J., Asner, G.P., Davies, S.J., Dehgan, A., Saatchi, S., 2014. These are the days
627 of lasers in the jungle. Carbon Balance Management, 9, (1),
628 7. DOI: 10.1186/s13021-014-0007-0
629 Melo, F.P.L., Pinto, S.R.R., Brancalion, P.H.S., Castro, P.S., Rodrigues, R.R., Aronson,
630 J., Tabarelli, M., 2013. Priority setting for scaling-up tropical forest restoration
631 projects: early lessons from the Atlantic Forest Restoration Pact. Environmental
632 Science and Policy, 33, 395–404. http://dx.doi.org/10.1016/j.envsci.2013.07.013
633 Michez, A., Piégay, H., Jonathan, L., Claessens, H., & Lejeune, P., 2016. Mapping of
634 riparian invasive species with supervised classification of Unmanned Aerial
635 System (UAS) imagery. International Journal of Applied Earth Observation and
636 Geoinformation, 44, 88-94. http://dx.doi.org/10.1016/j.jag.2015.06.014
637 Moreau, A.M.S.S., Ker, J.C., Costa, L.M., Gomes, F.H., 2006. Caracterização de solos
638 de duas toposequências em Tabuleiros Costeiros do Sul da Bahia. Revista
639 Brasileira de Ciência do Solo, 30, 1007-1019. (Abstract in English)
640 http://dx.doi.org/10.1590/S0100-06832006000600010
641 Movia, A., Beinat, A., Crosilla, F., 2016. Shadow detection and removal in RGB VHR
642 images for land use unsupervised classification. ISPRS Journal of

643 Photogrammetry and Remote Sensing, 119, 485-495.
644 https://doi.org/10.1016/j.isprsjprs.2016.05.004
645 Muñoz-Rojas, M., Erickson, T. E., Dixon, K. W. and Merritt, D. J., 2016. Soil quality
646 indicators to assess functionality of restored soils in degraded semiarid
647 ecosystems. Restor Ecol, 24: S43–S52. doi:10.1111/rec.12368
648 de Oliveira, F.P., Fernandes Filho, E. I., Soares, V.P., 2013. Mapeamento de fragmentos
649 florestais com monodominância de aroeira a partir da classificação
650 supervisionada de imagens RapidEye1. Revista Árvore, 37 (1), 151-161.
651 (Abstract in English) http://dx.doi.org/10.1590/S0100-67622013000100016.
652 Ockendon, N., Thomas, D.H.L., Cortina, J., Adams, W.M., Aykroyd, T.,Barov, B.,
653 Boitani, L., Bonn, A., Branquinho, C., Brombacher, M., Burrellm, C., Carvern,
654 S., Cricko, H.Q.P., Duguyp, B., Everettq, S., Fokkensr, B., Fullers,
655 R.J., Gibbonst, D. W., Gokhelashviliu, R., Griffinv, C., Halleyw, J.D., Hothamx,
656 P., Hughesy, F.M.R., Karamanlidisz, A.A., McOwenaa, C.J., Milesaa,
657 L., Mitchellab, R., Randsac, M.R.W, Robertsad, J., Sandomae, C.J., Spenceraf,
658 J.W, Broekeag. E., Tewb, E.R., Thomasah, C.D., Anastasiya Timoshynaai, A.,
659 Unsworthaj, R.K.F, Warringtonak, S., Sutherlandb, W.J.,2018. One hundred
660 priority questions for landscape restoration in Europe. Biological Conservation,
661 221, 198-208. https://doi.org/10.1016/j.biocon.2018.03.002
662 Paneque-Gálvez, J., McCall, M.K., Napoletano, B.M., Wich, S.A., & Koh, L.P, 2014.
663 Small drones for community-based forest monitoring: An assessment of their
664 feasibility and potential in tropical areas. Forests, 5 (6), 1481-1507. DOI:
665 10.3390/f5061481
666 Persson, A., Holmgren, J., Söderman, U., Olsson, H., 2004. Tree species classification
667 of individual trees in Sweden by combining high resolution laser data with high
668 resolution near-infrared digital images. International Archives of
669 Photogrammetry, Remote Sensing and Spatial Information Sciences, 36 (8),
670 204-207.
671 Puissant, A., Rougier, S., Stumpf, A., 2014. Object-oriented mapping of urban trees
672 using Random Forest classifiers. International Journal of Applied Earth
673 Observation and Geoinformation, 26, 235-245.
674 http://dx.doi.org/10.1016/j.jag.2013.07.002

675 R Core Team, 2016. R: A language and environment for statistical computing. R
676 Foundation for Statistical Computing, Vienna, Austria. URL http://www.R-
677 project.org/.
678 Reif, M.K., Theel, H.J., 2017. Remote sensing for restoration ecology: application for
679 restoring degraded, damaged, transformed, or destroyed ecosystems Integr.
680 Environ. Assess. Manag., 13, 614–630. DOI 10.1002/ieam.1847
681 Rouse, J.W., Haas, R.H., Schell, J.A., Deering, D.W., 1973. Monitoring vegetation
682 systems in the Great Plains with ERTS. In3rd ERTS Symposium, NASA SP-351
683 I, 309–317.
684 Rocha-Nicoleite, E., Overbeck, G.E., Müller, S.C., 2017. Degradation by coal mining
685 should be priority in restoration planning. Perspect. Ecol. Conserv. 15, 197–200.
686 https://doi.org/10.1016/j.pecon.2017.05.006
687 Rodrigues, R.R., Lima, R.A., Gandolfi, S., Nave, A. G., 2009. On the restoration of
688 high diversity forests: 30 years of experience in the Brazilian Atlantic Forest.
689 Biological conservation, 142(6), 1242-1251. DOI:10.1016/j.biocon.2008.12.008
690 Ruiz-Jaen, M.C., Aide, T.M., 2005. Restoration Success: How is it being measured?
691 Restoration Ecology, 13, 569 -577. DOI: 10.1111/j.1526-100X.2005.00072.x
692 Saporetti Junior, A.W., Schaefer, C.E.G.R., Souza, A.L., Soares, M.P., Araújo, D.S.D.,
693 Meira-Neto J.A.A., 2012. Influence of soil physical properties on plants of
694 Mussununga ecosystem, Brazil. Folia Geobot, 47, 29-39. DOI 10.1007/s12224-
695 011-9106-9
696 Silva, F.C.M., Silva, N. M., Cândido, A.K.A.A., 2016. Seleção de técnicas de
697 classificação de fotografias aéreas derivadas de VANT na análise ambiental de
698 área de cerrado. REDE-Revista Eletrônica do PRODEMA, 10 (1), 74-84.
699 (Abstract in English)
700 Song, J. H., Han, S. H., Yu, K. Y., Kim, Y.I., 2002. Assessing the possibility of land-
701 cover classification using LIDAR intensity data. International Archives of
702 Photogrammetry Remote Sensing and Spatial Information Sciences, 34 (3/B),
703 259-263.
704 Thenkabail, P.S., Enclona, E.A., Ashton, M.S., Legg, C. and De Dieu, M.J., 2004.
705 Hyperion, IKONOS, ALI, and ETM+ sensors in the study of African rainforests.
706 Remote Sensing of Environment, 90, 23-43. DOI:10.1016/j.rse.2003.11.018

Veloso, H.P., Rangel Filho, A.L.R., Lima, J.C.A., 1991. Classificação da vegetação brasileira adaptada a um sistema universal. Rio de Janeiro: IBGE, Departamento de Recursos Naturais e Estudos Ambientais. 124 p.

Viani, R.A., Holl, K.D., Padovezi, A., Strassburg, B.B., Farah, F.T., Garcia, L.C., Chaves, R.B., Rodrigues, R.R., Brancalion, P. H., 2017. Protocol for monitoring tropical forest restoration: perspectives from the Atlantic forest restoration pact in Brazil. Tropical Conservation Science, 10, https://doi.org/10.1177/1940082917697265

Xian, G., Homer, C., Fry, J., 2009. Updating the 2001 National Land Cover Database land cover classification to 2006 by using Landsat imagery change detection methods. Remote Sensing of Environment, 113(6), 1133-1147. DOI:10.1016/j.rse.2009.02.004

Zahawi, R.A., Dandois, J.P., Holl, K.D., Nadwodny, D., Reid, J. L., Ellis, E. C., 2015. Using lightweight unmanned aerial vehicles to monitor tropical forest recovery. Biological Conservation, 186, 287-295. http://dx.doi.org/10.1016/j.biocon.2015.03.031

Zlinszky, A., Schroiff, A., Kania, A.,Deak, B., Mücke, W., Vari, A., Szekely, B., Pfeifer, N., 2014. Categorizing grassland vegetation with full-waveform airborne laser scanning: a feasibility study for detecting Natura 2000 habitat types. Remote Sens., 6 , 8056-8087. DOI:10.3390/rs6098056

Zonete, M.F., Rodriguez, L.C.E., Packalén, P., 2010. Estimação de parâmetros biométricos de plantios clonais de eucalipto no sul da Bahia: uma aplicação da tecnologia laser aerotransportada. Scientia Forestalis, 38 (86), 225-235. (Abstract in English)